Supporting Information for

Palaeo-seawater density reconstruction and its implication for cold-water coral carbonate mounds in the northeast Atlantic through time

Andres Rüggeberg[1,2,3*], Sascha Flögel[2], Wolf-Christian Dullo[2], Jacek Raddatz[2,4], Volker Liebetrau[2]

[1] Dept. of Geosciences, University of Fribourg, Chemin du Musée 6, CH-1700 Fribourg, Switzerland.
[2] GEOMAR Helmholtz Centre for Ocean Research Kiel, Wischhofstr. 1-3, D-24148 Kiel, Germany.
[3] Renard Centre of Marine Geology, Ghent University, Krijgslaan 281, S8, B-9000 Gent, Belgium.
[4] Present address: Institute of Geosciences, Goethe University Frankfurt, Altenhöferallee 1, D-60438, Frankfurt am Main, Germany

* To whom correspondence should be addressed. Email: andres.rueggeberg@unifr.ch

Contents of this file

Supporting Text S1.

Uranium isotope analyses

U-Th measurements of the sample set (Table S1) were performed on a Finnigan MAT 262 RPQ+ (Mat262, U) and a Thermo-Finnigan Triton-RPQ (Triton, U) thermal ionisation mass spectrometer (TIMS) and a VG Axiom multi collector - inductively coupled plasma - mass spectrometer (MC-ICP-MS, including multi ion counting (MIC) set-up). The $\delta^{234}U_{(0)}$ value represents the originally today measured ($^{234}U/^{238}U$) activity ratio, given in delta notation ($\delta^{234}U_{(0)} = (((^{234}U_{act}/^{238}U_{act})-1) * 1000$). Displayed $\delta^{234}U_{(T)}$ values reflect age corrected ($^{234}U/^{238}U$) activity ratios by recalculating the decay of ^{234}U for the time interval T ($\delta^{234}U_{(T)} = \delta^{234}U_{(0)}exp^{(\lambda 234 T)}$), determined from $^{230}Th/^{234}U$ age of each individual sample. Note, due to the generally high ages in this sample set, the impact of age correction on the interpretation of $\delta^{234}U$ values is significant and criteria for isotopic reliability of ^{230}Th age data may be applied. Recent reef forming cold-water corals showed within their uncertainties similar $\delta^{234}U_{(0)}$ values of 145.5 ± 2.3 ‰ [Cheng et al., 2000] and 146.3 ± 3.9 ‰ [Liebetrau et al., 2010], supporting the application of the $\delta^{234}U_{(T)}$ reliability criterion presented for tropical [Blanchon et al., 2009] or cold-water corals [Wienberg et al., 2010]. $\delta^{234}U_{(T)}$ criterion and related U-Th age quality code: n = not reliable (potential diagentic overprint) , R = reliable: passing the 149 ± 10 ‰ $\delta^{234}U_{(T)}$

criterion [see also Stirling et al., 1998; Robinson et al., 2004; Esat and Yokoyama, 2006]; SR = strictly reliable: within 146.6 - 149.6 ‰ $\delta^{234}U_{(T)}$, representing values for modern corals and modern seawater, respectively [Delanghe et al., 2002; Robinson et al., 2004] (Fig. S1). First order classification is disregarding the individual analytical uncertainty, avoiding preference to less precise measurements. Maximum quality level reached within range of analytical uncertainty is indicated in brackets (Table S1).

References

Blanchon, P., A. Eisenhauer, J. Fietzke, and V. Liebetrau (2009), Rapid sea-level rise and reef back-stepping at the close of the last interglacial highstand, Nature, 458, 881–885.

Cheng, H., J. Adkins, R. L. Edwards, and E. A. Boyle (2000), U-Th dating of deep-sea corals, Geochimica et Cosmochimica Acta, 64(14), 2401–2416.

Delanghe, D., E. Bard, and B. Hamelin (2002), New TIMS constraints on the uranium-238 and uranium-234 in seawaters from the main ocean basins and the Mediterranean Sea, Marine Chemistry, 80, 79–93.

Esat, T. M., and Y. Yokoyama (2006), Variability in the uranium isotopic composition of the oceans over glacial–interglacial timescales, Geochimica et Cosmochimica Acta, 70, 4140–4150.

Liebetrau, V., A. Eisenhauer, and P. Linke (2010), Cold seep carbonates and associated cold-water corals at the Hikurangi Margin, New Zealand: New insights into fluid pathways, growth structures and geochronology, Marine Geology, 272, 307–318.

Robinson, L. F., N. S. Belshaw, and G. M. Henderson (2004), U and Th concentrations and isotope ratios in modern carbonates and waters from the Bahamas, Geochimica et Cosmochimica Acta, 68(8), 1777–1789.

Stirling, C. H., T. M. Esat, K. Lambeck, M. T. McCulloch (1998), Timing and duration of the Last Interglacial: evidence for a restricted interval of widespread coral reef growth, Earth and Planetary Science Letters, 160, 745–762.

Wienberg, C., et al. (2010), Glacial cold-water coral growth in the Gulf of Cádiz: Implications of increased palaeo-productivity, Earth and Planetary Science Letters 298, 405–416.

Supporting Text S2.

Stable oxygen isotope analyses of seawater

Water samples from the Porcupine Seabight were collected during expeditions of the RV METEOR and RV POSEIDON in April (M61/1), June (M61/3) and August (P316) 2004 (Table S2). Water samples for isotope analysis were filled into 100 ml crimp sealed glass bottles and 0.2 ml of a saturated $HgCl_2$ solution was added to stop biological activity. Oxygen isotopes were analyzed at the Leibniz Laboratory at Kiel University (Germany) applying the CO_2-water isotope equilibration technique on 4 ml sub-samples on the Kiel Equi unit on-line coupled to a Finnigan Delta E isotope ratio mass spectrometer and on 0.5 ml sub-samples on a Finnigan gas bench II unit coupled to a Finnigan DeltaPlusXL [Bauch et al., 2005]. The $^{18}O/^{16}O$ ratio is given versus VSMOW in the usual δ-notation [Craig, 1961]. The measurement precision for $\delta^{18}O$ analysis is ±0.05 ‰, respectively.

The thermohaline gradient within the water column, internal waves at depth, and different seasons during sampling account for the wider spread of the $\delta^{18}O_{sw}$ results from water depths of carbonate mounds (Table S2, Fig. S2). Additionally, due to the small salinity range of ΔS < 0.3 psu for our data and the concentration of samples from coral reef sites, the correlation coefficient is rather low (Fig. S2). However, in comparison to the Global Seawater $\delta^{18}O$ Dataset [Schmidt et al., 1999] for the NE Atlantic region our linear relation between $\delta^{18}O_{sw}$ and salinity is supported.

References

Bauch, D., H. Erlenkeuser, and N. Andersen (2005), Water mass processes on Arctic shelves as revealed from $\delta^{18}O$ of H_2O, Global and Planetary Change, 48, 165–174.

Craig, H. (1961), Standard for reporting concentrations of deuterium and oxygen 18 in natural waters, Science, 133, 1833–1834.

Schmidt, G. A., G. R. Bigg, and E. J. Rohling (1999), Global Seawater Oxygen-18 Database, http://data.giss.nasa.gov/o18data/.

Supporting Text S3.

Stable oxygen isotope analyses of benthic foraminifera

After cutting the cores of GeoB 6730-1, sediment samples were taken in intervals of 5 cm. Sediment samples of IODP Site U1317C were taken every ~10 cm at the IODP Core Repository at Bremen University, Germany [Raddatz et al., 2011].

Stable oxygen isotope analyses were carried out on 3 to 5 individuals of the benthic foraminifera *Cibicidoides kullenbergi* and/or *Cibicidoides wuellerstorfi* for GeoB 6730-1 (Table S4), and of *Lobatula lobatula* and/or *C. wuellerstorfi* for IODP core U1317C (Table S5), selected from the fraction 250 to 500 µm. The isotopic composition of foraminiferal tests was analyzed at the University of Bremen Isotope Lab for GeoB 6730-1 [Dorschel et al., 2005] and at IFM-GEOMAR in Kiel and Isotope Laboratory of the Institute of Geology and Mineralogy at the University of Erlangen for IODP core U1317C [Raddatz et al., 2011]. Samples were reacted at 75°C with phosphoric acid in a Kiel 182 CARBO device linked to a Finnigan MAT 251 (Bremen) or Finnigan MAT 252 (Kiel/Erlangen) mass spectrometer. For all $\delta^{18}O_C$ measurements a working standard (Burgbrohl CO_2 gas) was used and calibrated against PDB (Peedee Belemnite) by using the NBS (National Bureau of Standards) 18, 19, and 20 standards. Analytical standard deviation resulted in ±0.07 ‰ PDB for MAT 251 and ±0.05 ‰ PDB for MAT 252 instruments.

Previous studies already reported that the stable isotopic ratios of *C. wuellerstorfi* and *C. kullenbergi* are indistinguishable within analytical error [Hodell et al., 2001]. In our studied cores of Propeller Mound [Rüggeberg et al., 2007; Dorschel et al., 2005], paired analyses of these species also indicate a 1:1 relation in $\delta^{18}O_C$ (Fig. S3, Table S6). The same holds true for *C. wuellerstorfi* and *L. lobatulus* of IODP core U1317C as shown in the downcore record of Raddatz et al. [2011].

Paleotemperature estimates are based on the recently developed equation of Marchitto et al. [2014] leading to reconstructed temperatures of 9.3–10.0°C for the Holocene, 7.2–8.4°C for MIS 5, 4.0–7.9°C for MIS 6.5, 6.8–8.9°C for MIS 7, 4.3–8.6°C for MIS 9, 7.4–11.9°C for the Early Pleistocene, and 15.4–18.1°C for the Middle Miocene (see Table S4, S5). These estimates are in

agreement with published data using different methods [e.g., Peck et al., 2008; Raddatz et al., 2011, 2014; Khélifi et al., 2009, 2014].

References

Dorschel, B., D. Hebbeln, A. Rüggeberg, W.-C. Dullo, and A. Freiwald (2005), Growth and erosion of a cold-water coral covered carbonate mound in the Northeast Atlantic during the Late Pleistocene and Holocene, Earth and Planetary Science Letters, 233, 33–44.

Hodell, D.A., J.H. Curtis, F.J. Sierro, and M.E. Raymo (2001), Correlation of late Miocene to early Pliocene sequences between the Mediterranean and North Atlantic, Paleoceanography, 16, 164–178.

Khélifi, N., M. Sarnthein, N. Andersen, T. Blanz, M. Frank, D. Garbe-Schönberg, B. A. Haley, R. Stumpf, M. Weinelt (2009), A major and long-term Pliocene intensification of the Mediterranean outflow, 3.5–3.3 Ma ago, Geology, 37(9), 811–814.

Khélifi, N., M. Sarnthein, M. Frank, N. Andresen, and D. Garbe-Schönberg (2014), Late Pliocene variations of the Mediterranean outflow, Marine Geology, 357, 182–194.

Marchitto, T. M., W. B. Curry, J. Lynch-Stieglitz, S. P. Bryan, K. M. Cobb, and D. C. Lund (2014), Improved oxygen isotope temperature calibrations for cosmopolitan benthic foraminifera, Geochimica et Cosmochimica Acta, 130, 1–11.

Peck, V. L., I. R. Hall, R. Zahn, and H. Elderfield (2008), Millennial-scale surface and subsurface paleothermometry from the northeast Atlantic, 55–8 ka BP, Paleoceanography, 23, PA3221, doi:10.1029/2008PA001631.

Raddatz, J., A. Rüggeberg, S. Margreth, W.-Chr. Dullo, and IOPD Expedition 307 Scientific Party (2011), Paleoenvironmental reconstruction of Challenger Mound initiation in the Porcupine Seabight, NE Atlantic, Marine Geology, 282, 79–90.

Raddatz, J., A. Rüggeberg, V. Liebetrau, A. Foubert, E.C. Hathorne, J. Fietzke, A. Eisenhauer, and W.-Chr. Dullo (2014), Environmental boundary conditions of cold-water coral mound growth over the last 3 million years in the Porcupine Seabight, Northeast Atlantic, Deep-Sea Research II, 99, 227–236.

Rüggeberg, A., C. Dullo, B. Dorschel, and D. Hebbeln (2007), Environmental changes and growth history of Propeller Mound, Porcupine Seabight: Evidence from benthic foraminiferal assemblages, International Journal of Earth Sciences, 96, 57–72.

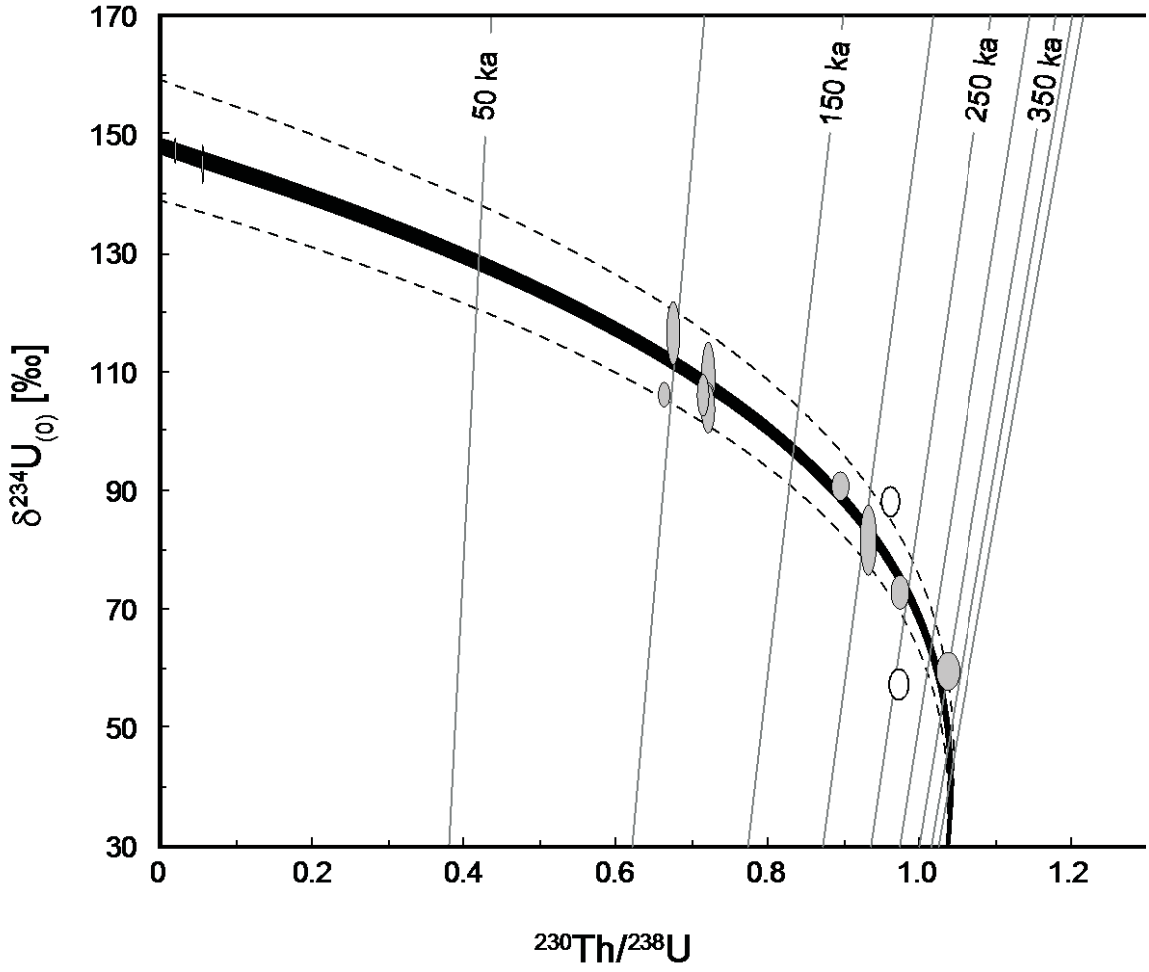

Figure S1. U-series evolution diagram of investigated coral samples (see Table S1). The solid black line represents the isotopic evolution of a closed system starting with a mean $\delta^{234}U_{(0)}$ of 147–149‰ and a zero $^{230}Th/^{238}U$ activity, while the dashed lines started with a mean $\delta^{234}U_{(0)}$ of 139‰ and 159‰ and a zero $^{230}Th/^{238}U$ activity, respectively. Deviations from this span are possibly due to diagenetic alteration as indicated by the white ellipses of samples 6730-1/213 and 6730-1/353 (Table S1).

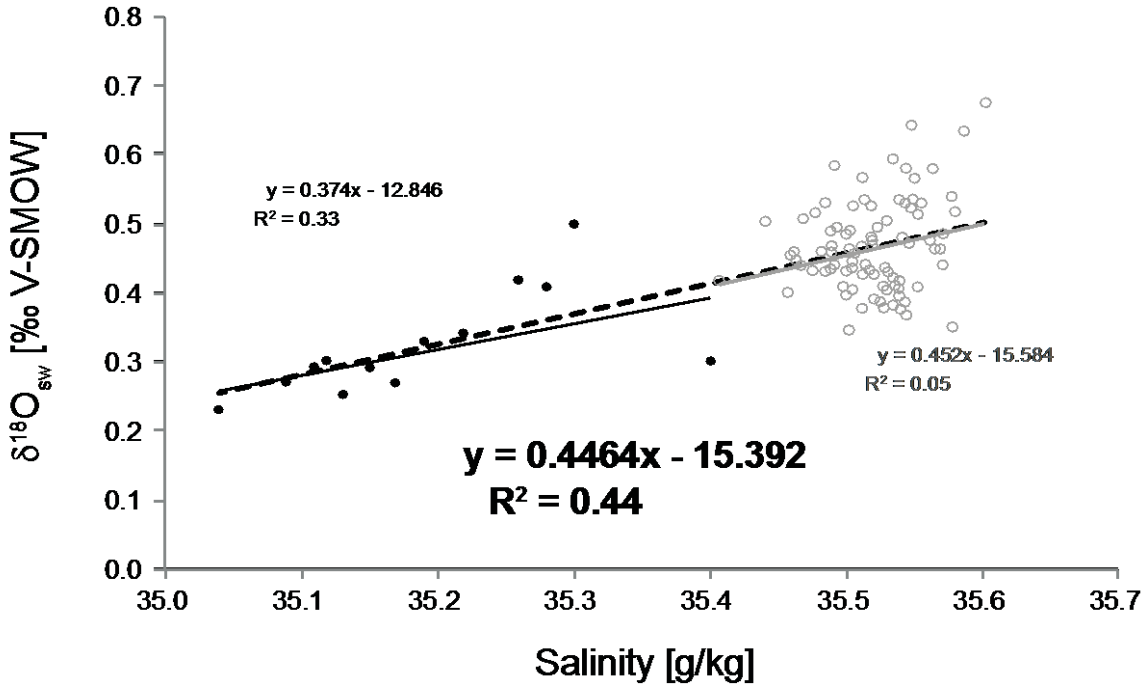

Figure S2. $\delta^{18}O_{SW}$–salinity relation of the upper water column (0–1155 m) from water samples collected during cruises M61/1, M61/3, P316 in summer 2004 (circles, this study, see Table S2) in comparison with data of the Global Seawater $\delta^{18}O$ Database (diamonds, Schmidt et al., 1999) for the NE Atlantic between 0–30°W, 30–60°N, and 10–1500 m.

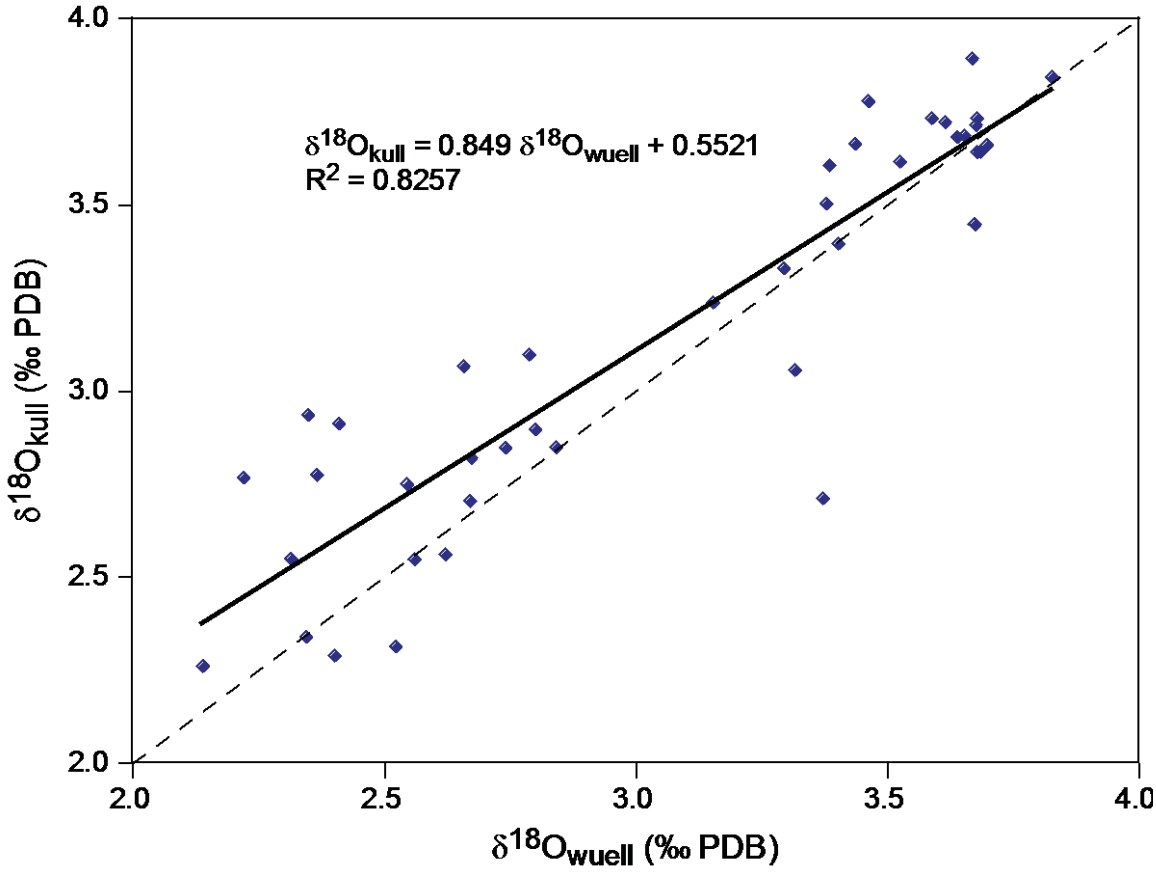

Figure S3. Linear relation between (a) $\delta^{18}O_C$ of *Cibicidoides kullenbergi* ($\delta^{18}O_{kull}$) and *Cibicidoides wuellerstorfi* ($\delta^{18}O_{wuell}$) from GeoB 6730-1 (Table S6) selected from fraction 250 to 500 µm. Dashed line indicates 1:1 relation between the paired $\delta^{18}O_C$ ratios.

Table S1. U and Th isotopes and calculated ages of cold-water corals from core GeoB 6730-1 (MIS = Marine Isotope Stage). All uncertainties are based on 2 SEM level of the isotope measurements. $\delta^{234}U_{(T)}$ reliability criterion and related U-Th age quality code follow Wienberg et al. [2010]: n = not reliable (potential diagentic overprint) , R = reliable (passing the 149 ± 10‰ $\delta^{234}U_{(T)}$ criterion); SR = strictly reliable (within 146.6 - 149.6‰ $\delta^{234}U_{(T)}$, representing values for modern corals and modern seawater, respectively). First order classification is disregarding the individual analytical uncertainty, avoiding preference to less precise measurements. Maximum quality level reached within range of analytical uncertainty is indicated in brackets. Applied MS: T = Triton, A1/2 = Axiom1/2, M = MAT262. * Mean values reflect reproducibility and robustness of applied methods. Uncertainties of mean values are given as 2 SEM. ** Nevertheless, despite precise isotope measurements, for sample 318 enlarged age uncertainty and less age reliability must be deduced due to high Th concentrations (> 100 ng g^{-1}) and the related uncertainty of correction for potential detrital impact. *** No reasonable classification possible.

sample ident (GeoB core / depth in cm)	applied MS (U/Th)	Weight (g)	^{238}U-conc. (µg/g)	^{232}Th conc. (µg/g)	^{230}Th (pg/g)	^{230}Th/^{232}Th act. ratio	^{230}Th/^{234}U act. ratio	$\delta^{234}U_{(0)}$ (‰)	$\delta^{234}U_{(T)}$	**U-Th age (ky BP)**	+/- (‰)	$\delta^{234}U_{(T)}$ criterion	**MIS**
6730-1/3	Triton/Axiom	0.224	4.15 ± *0.02*	14.6 ± *0.1*	1.4 ± *0.1*	17.7 ± *0.8*	0.017 ± *0.001*	147.3 ± *1.8*	148.1 ± *1.8*	**1.9 ± *0.1***	*4.7*	SR	**1**
6730-1/18	Triton/Axiom	0.243	4.64 ± *0.02*	53.3 ± *0.3*	4.3 ± *0.1*	15.0 ± *0.2*	0.047 ± *0.001*	145.0 ± *2.7*	147.2 ± *2.7*	**5.2 ± *0.1***	*2.1*	SR	**1**
6730-1/58	Triton/Axiom1	0.320	4.78 ± *0.02*	12.3 ± *0.1*	52.8 ± *0.3*	802.3 ± *6.5*	0.603 ± *0.005*	116.7 ± *4.3*	154.2 ± *5.1*	**99 ± *1***	*1.4*	R (SR)	**5.3**
6730-1/68	Triton/Axiom	0.273	4.57 ± *0.02*	79.2 ± *0.4*	49.6 ± *0.3*	117.3 ± *0.9*	0.595 ± *0.004*	106.4 ± *1.7*	139.9 ± *2.2*	**97 ± *1***	*1.1*	n (R)	**5.3**
6730-1/108	Mat262/Axiom2	0.192	3.94 ± *0.02*	1.05 ± *0.1*	46.5 ± *0.2*	8327 ± *57.3*	0.650 ± *0.005*	108.9 ± *5.1*	149.4 ± *6.0*	**112 ± *2***	*1.3*	SR	**5.5**
6730-1/108	Triton/Axiom1	0.192	3.94 ± *0.02*	1.30 ± *0.1*	46.5 ± *0.3*	6696 ± *53.6*	0.651 ± *0.005*	106.0 ± *1.9*	145.6 ± *2.6*	**112 ± *1***	*1.2*	R (SR)	**5.5**
6730-1/108	Axiom/Axiom2	0.192	3.98 ± *0.02*	1.05 ± *0.1*	46.5 ± *0.2*	8327 ± *57.3*	0.647 ± *0.004*	104.0 ± *3.2*	142.3 ± *3.9*	**111 ± *1***	*1.2*	R	**5.5**
6730-1/108	mean*	0.192	3.95 ± *0.03*	1.20 ± *0.3*	46.5 ± *0.04*	7512 ± *1631*	0.649 ± *0.003*	106.3 ± *2.86*	145.8 ± *4.14*	**112 ± *1***	*0.7*	R (SR)	**5.5**
6730-1/178	Triton/Axiom	0.148	2.91 ± *0.01*	58.4 ± *0.3*	42.6 ± *031*	136.5 ± *1.1*	0.815 ± *0.006*	91.1 ± *2.0*	149.8 ± *3.4*	**176 ± *3***	*1.8*	R (SR)	**6.5**
6730-1/213	Triton/Axiom	0.169	2.86 ± *0.01*	26.4 ± *0.1*	45.1 ± *0.2*	320.5 ± *2.3*	0.881 ± *0.006*	88.5 ± *2.0*	163.7 ± *4.2*	**218 ± *4***	*2.1*	n	***
6730-1/238	Triton/Axiom	0.566	3.68 ± *0.02*	1.13 ± *0.1*	56.1 ± *0.3*	9272 ± *63.0*	0.860 ± *0.007*	82.0 ± *4.8*	145.8 ± *7.0*	**204 ± *5***	*2.2*	R (SR)	**7.2**
6730-1/273	Axiom/Axiom	0.186	3.94 ± *0.02*	14.7 ± *0.1*	62.8 ± *0.3*	798.0 ± *5.6*	0.905 ± *0.006*	73.3 ± *2.3*	144.4 ± *4.8*	**240 ± *6***	*2.4*	R (SR)	**7.5**
6730-1/318**	Axiom/Axiom	0.298	3.34 ± *0.01*	390 ± *2.4*	56.6 ± *0.4*	27.2 ± *0.3*	0.950 ± *0.012*	60.0 ± *2.6*	139.4 ± *9.9*	**296 ± *18***	*6.1*	n (SR)	**8.5 - 9.1**
6730-1/353	Axiom/Axiom	0.018	4.65 ± *0.02*	31.6 ± *0.2*	73.9 ± *0.4*	438.8 ± *3.9*	0.916 ± *0.007*	57.8 ± *2.1*	118.7 ± *4.9*	**254 ± *8***	*3.1*	n	***

Table S2. CTD data of temperature, salinity, density and depth, and $\delta^{18}O_{SW}$ measurements of water samples from the upper water column (0–1155 m) collected during cruises M61/1, M61/3, P316 in summer 2004. These data were used to determine regional $\delta^{18}O_{SW}$–salinity relation (Eq. 1), to calculate theoretical $\delta^{18}O_C$ (Eq. 2) and then determine $\sigma_\theta - \delta^{18}O_C$ relation (Eq. 3). Uncertainties between measured and calculated data: $\Delta^{18}O_{SW}$ = measured $\delta^{18}O_{SW}$ – calculated $\delta^{18}O_{SW}$ (in ‰ V-SMOW) and $\Delta\sigma_\theta$ = measured σ_θ – calculated σ_θ (in kg m^{-3}).

Porcupine Seabight Cruise	Station	Area	Latitude [N]	Longitude [W]	Depth [m]	Temp. [°C]	Salinity [g/kg]	$\delta^{18}O_{SW}$ [‰ V-SMOW]	σ_θ [kg/m^3]		Eq. 1 $\delta^{18}O_{SW}$	$\Delta^{18}O_{SW}$	Eq. 2 $\delta^{18}O_C$	Eq. 3 σ_θ	$\Delta\sigma_\theta$
M61/3	588	N of Propeller Mound. HMP	52°09.34'	12°45.95'	790	9.59	35.51	0.46	27.43		0.46	0.00	1.57	27.42	0.01
M61/3	589	Top Propeller Mound. HMP	52°08.89'	12°46.27'	705	9.94	35.46	0.45	27.34		0.44	-0.01	1.48	27.35	-0.01
M61/3	589	Top Propeller Mound. HMP	52°08.89'	12°46.27'	598	10.00	35.41	0.42	27.28		0.41	0.00	1.44	27.32	-0.04
M61/3	589	Top Propeller Mound. HMP	52°08.89'	12°46.27'	432	10.73	35.48	0.52	27.20		0.45	-0.07	1.37	27.27	-0.06
M61/3	589	Top Propeller Mound. HMP	52°08.89'	12°46.27'	337	11.16	35.55	0.56	27.18		0.48	-0.09	1.33	27.23	-0.04
M61/3	589	Top Propeller Mound. HMP	52°08.89'	12°46.27'	256	11.21	35.55	0.64	27.17		0.48	-0.16	1.39	27.28	-0.11
M61/3	589	Top Propeller Mound. HMP	52°08.89'	12°46.27'	189	11.33	35.57	0.58	27.16		0.48	-0.09	1.30	27.21	-0.05
M61/3	589	Top Propeller Mound. HMP	52°08.89'	12°46.27'	92	11.53	35.59	0.63	27.14		0.49	-0.14	1.31	27.21	-0.08
M61/3	589	Top Propeller Mound. HMP	52°08.89'	12°46.27'	38	12.09	35.60	0.67	27.05		0.50	-0.17	1.23	27.14	-0.09
M61/3	590	S of Propeller Mound. HMP	52°08.24'	12°46.41'	708	9.77	35.49	0.53	27.39		0.45	-0.08	1.60	27.44	-0.06
M61/1	233	Galway Mound. BMP	51°27.02'	11°48.95'	8	11.34	35.55	0.41	27.15		0.48	0.07	1.13	27.06	0.10
M61/1	283-2	SW of Galway Mound. BMP	51°23.86'	11°48.58'	30	11.49	35.54	0.53	27.13		0.47	-0.06	1.22	27.14	-0.01
M61/1	233	Galway Mound. BMP	51°27.02'	11°48.95'	38	11.21	35.54	0.48	27.17		0.47	-0.01	1.23	27.15	0.02
M61/1	233	Galway Mound. BMP	51°27.02'	11°48.95'	120	11.18	35.55	0.51	27.18		0.48	-0.03	1.27	27.18	0.00
M61/1	233	Galway Mound. BMP	51°27.02'	11°48.95'	175	11.11	35.54	0.53	27.19		0.47	-0.05	1.30	27.20	-0.02
M61/1	233	Galway Mound. BMP	51°27.02'	11°48.95'	250	11.07	35.54	0.58	27.19		0.47	-0.10	1.36	27.26	-0.07
M61/1	283-2	SW of Galway Mound. BMP	51°23.86'	11°48.58'	250	10.96	35.53	0.50	27.20		0.47	-0.03	1.31	27.21	-0.01
M61/1	233	Galway Mound. BMP	51°27.02'	11°48.95'	430	10.82	35.50	0.53	27.22		0.46	-0.07	1.36	27.26	-0.04
M61/1	283-2	SW of Galway Mound. BMP	51°23.86'	11°48.58'	500	10.68	35.49	0.47	27.22		0.45	-0.01	1.33	27.23	-0.01
M61/1	233	Galway Mound. BMP	51°27.02'	11°48.95'	559	10.35	35.44	0.50	27.27		0.43	-0.07	1.44	27.32	-0.06
M61/1	233	Galway Mound. BMP	51°27.02'	11°48.95'	665	9.76	35.46	0.40	27.34		0.44	0.04	1.47	27.35	0.00
M61/1	280-2	S of Poseidon Mound. BMP	51°24.36'	11°41.36'	680	10.00	35.47	0.44	27.33		0.44	0.00	1.46	27.34	-0.01
M61/1	283-2	SW of Galway Mound. BMP	51°23.86'	11°48.58'	750	9.75	35.46	0.45	27.37		0.44	-0.02	1.53	27.39	-0.02
M61/1	209	Galway Mound. BMP	51°27.09'	11°45.12'	786	9.96	35.47	0.51	27.36		0.44	-0.06	1.54	27.39	-0.03

M61/1	233	Galway Mound. BMP	51°27.02'	11°48.95'	795	9.52	35.53	0.41	27.42		0.47	0.06	1.54	27.40	0.02
M61/1	208	Galway Mound. BMP	51°27.26'	11°45.19'	806	9.79	35.49	0.46	27.39		0.45	-0.01	1.53	27.39	0.00
M61/1	229	Galway Mound. BMP	51°27.08'	11°45.14'	809	9.68	35.49	0.49	27.40		0.45	-0.04	1.58	27.43	-0.02
M61/1	252	Thérèse Mound. BMP	51°25.70'	11°46.29'	850	9.28	35.54	0.41	27.51		0.47	0.06	1.59	27.44	0.07
M61/1	211	Galway Mound. BMP	51°26.80'	11°45.19'	865	9.40	35.52	0.43	27.48		0.46	0.03	1.58	27.43	0.04
M61/1	207	Galway Mound. BMP	51°27.44'	11°45.30'	868	9.51	35.50	0.40	27.45		0.46	0.06	1.53	27.39	0.06
M61/1	230	Galway Mound. BMP	51°27.10'	11°45.29'	873	9.28	35.52	0.47	27.50		0.46	-0.01	1.66	27.48	0.01
M61/1	213	Little Galway Mound. BMP	51°26.38'	11°45.48'	880	9.09	35.53	0.41	27.51		0.47	0.06	1.63	27.47	0.04
M61/1	214	Little Galway Mound. BMP	51°26.53'	11°45.42'	880	9.22	35.52	0.43	27.54		0.46	0.04	1.62	27.46	0.07
M61/1	228	Galway Mound. BMP	51°27.13'	11°44.91'	884	9.63	35.52	0.47	27.44		0.46	0.00	1.57	27.42	0.01
M61/1	233	Galway Mound. BMP	51°27.02'	11°48.95'	884	9.01	35.52	0.44	27.53		0.46	0.02	1.68	27.50	0.02
M61/1	212	Galway Mound. BMP	51°26.69'	11°45.18'	893	9.27	35.52	0.43	27.50		0.46	0.03	1.62	27.46	0.04
M61/1	279	Pollux Mound. BMP	51°24.97'	11°45.97'	905	8.56	35.53	0.43	27.60		0.47	0.04	1.78	27.57	0.03
M61/1	254	Thérèse Mound. BMP	51°25.94'	11°46.23'	907	8.94	35.54	0.37	27.57		0.47	0.11	1.63	27.46	0.11
M61/1	253	Thérèse Mound. BMP	51°25.82'	11°46.31'	910	9.03	35.54	0.40	27.55		0.47	0.08	1.63	27.47	0.09
M61/1	205	Galway Mound. BMP	51°27.85'	11°45.07'	914	9.30	35.50	0.43	27.48		0.46	0.02	1.61	27.45	0.03
M61/1	227	Galway Mound. BMP	51°27.17'	11°44.43'	917	9.59	35.52	0.48	27.46		0.46	-0.02	1.59	27.44	0.02
M61/1	251	Thérèse Mound. BMP	51°25.52'	11°46.34'	919	8.72	35.53	0.38	27.59		0.47	0.09	1.69	27.51	0.09
M61/1	231	Galway Mound. BMP	51°27.08'	11°45.63'	946	9.10	35.54	0.40	27.55		0.47	0.07	1.63	27.46	0.09
M61/1	250	Thérèse Mound. BMP	51°25.37'	11°46.34'	960	8.70	35.54	0.42	27.60		0.47	0.05	1.73	27.54	0.07
M61/1	232	Galway Mound. BMP	51°27.11'	11°45.37'	973	8.87	35.54	0.42	27.58		0.47	0.06	1.69	27.51	0.07
M61/1	255	Thérèse Mound. BMP	51°26.15'	11°46.27'	989	8.71	35.54	0.38	27.60		0.47	0.09	1.69	27.51	0.09
M61/1	249	Thérèse Mound. BMP	51°25.15'	11°46.32'	995	8.65	35.53	0.44	27.61		0.47	0.03	1.76	27.56	0.05
M61/1	283-2	SW of Galway Mound. BMP	51°23.86'	11°48.58'	1002	8.81	35.54	0.38	27.59		0.47	0.10	1.66	27.49	0.10
M61/1	233	Galway Mound. BMP	51°27.02'	11°48.95'	1027	8.48	35.50	0.41	27.63		0.45	0.05	1.77	27.56	0.07
M61/1	233	Galway Mound. BMP	51°27.02'	11°48.95'	1051	8.21	35.48	0.46	27.65		0.45	-0.01	1.88	27.64	0.01
M61/1	278	N of Castor Mound. BMP	51°26.47'	11°47.24'	1058	8.75	35.54	0.42	27.60		0.47	0.05	1.72	27.53	0.07
M61/1	233	Galway Mound. BMP	51°27.02'	11°48.95'	1066	8.28	35.50	0.49	27.643		0.46	-0.03	1.89	27.65	-0.01
M61/1	283-2	SW of Galway Mound. BMP	51°23.86'	11°48.58'	1131	8.08	35.49	0.43	27.68		0.45	0.02	1.88	27.64	0.04
M61/1	283-2	SW of Galway Mound. BMP	51°23.86'	11°48.58'	1155	8.20	35.50	0.44	27.65		0.46	0.02	1.86	27.63	0.03
M61/3	585	Top of Galway Mound. BMP	51°27.08'	11°45.16'	786	9.47	35.55	0.39	27.48		0.48	0.09	1.53	27.39	0.10

M61/3	582	Top of Galway Mound. BMP	51°27.10'	11°45.22'	808	9.39	35.56	0.48	27.51		0.48	0.01	1.63	27.47	0.04
M61/3	579	Top of Galway Mound. BMP	51°26.98'	11°45.10'	822	9.18	35.57	0.46	27.56		0.49	0.02	1.67	27.49	0.07
M61/3	548	Top of Galway Mound. BMP	51°27.10'	11°45.06'	830	9.55	35.53	0.59	27.46		0.47	-0.12	1.71	27.53	-0.07
M61/3	547	S of Galway Mound. BMP	51°26.75'	11°45.11'	880	9.22	35.51	0.47	27.55		0.46	-0.01	1.66	27.49	0.06
M61/3	554	N of Galway Mound. BMP	51°27.60'	11°45.31'	908	9.35	35.55	0.54	27.53		0.48	-0.06	1.70	27.52	0.02
M61/3	580	E of Galway Mound. BMP	51°27.13'	11°44.57'	917	8.97	35.57	0.46	27.58		0.49	0.02	1.71	27.53	0.06
M61/3	562	E of Galway Mound. BMP	51°27.18'	11°44.33'	917	9.25	35.55	0.52	27.52		0.48	-0.05	1.71	27.52	0.00
M61/3	583	E of Galway Mound. BMP	51°27.22'	11°44.39'	919	8.96	35.58	0.35	27.59		0.49	0.14	1.61	27.45	0.15
M61/3	555	W of Galway Mound. BMP	51°27.13'	11°45.44'	920	9.19	35.56	0.53	27.54		0.48	-0.05	1.73	27.54	0.00
M61/3	578	W of Galway Mound. BMP	51°27.03'	11°45.82'	962	9.03	35.57	0.44	27.58		0.49	0.05	1.68	27.50	0.08
M61/3	584	W of Galway Mound. BMP	51°27.08'	11°45.78'	964	9.08	35.58	0.52	27.58		0.49	-0.03	1.74	27.55	0.03
M61/3	581	W of Galway Mound. BMP	51°26.98'	11°45.93'	974	8.95	35.57	0.49	27.59		0.49	0.00	1.74	27.55	0.04
P316	515	Top of Galway Mound. BMP	51°27.11'	11°45.17'	119	11.51	35.58	0.54	27.14		0.49	-0.05	1.22	27.14	-0.01
P316	515	Top of Galway Mound. BMP	51°27.11'	11°45.17'	345	11.14	35.55	0.47	27.18		0.48	0.01	1.24	27.15	0.03
P316	515	Top of Galway Mound. BMP	51°27.11'	11°45.17'	466	10.90	35.52	0.54	27.21		0.46	-0.07	1.35	27.25	-0.04
P316	515	Top of Galway Mound. BMP	51°27.11'	11°45.17'	530	10.68	35.49	0.44	27.24		0.45	0.01	1.31	27.21	0.02
P316	515	Top of Galway Mound. BMP	51°27.11'	11°45.17'	594	10.28	35.46	0.46	27.28		0.44	-0.02	1.42	27.30	-0.02
P316	536	Top of Poseidon Mound. BMP	51°27.44'	11°42.00'	691	9.36	35.51	0.56	27.47		0.46	-0.10	1.73	27.54	-0.06
P316	538	E of Poseidon Mound. BMP	51°27.49'	11°40.66'	728	9.84	35.49	0.58	27.38		0.45	-0.13	1.64	27.47	-0.10
P316	515	Top of Galway Mound. BMP	51°27.11'	11°45.17'	731	9.91	35.48	0.43	27.35		0.44	0.01	1.47	27.34	0.01
P316	537	E of Poseidon Mound. BMP	51°27.37'	11°41.73'	732	9.57	35.50	0.49	27.43		0.46	-0.03	1.61	27.45	-0.01
P316	535	W of Poseidon Mound. BMP	51°27.39'	11°42.39'	807	9.68	35.49	0.50	27.41		0.45	-0.04	1.59	27.43	-0.03
P316	517	S of Galway Mound. BMP	51°26.90'	11°45.12'	812	9.19	35.53	0.38	27.54		0.47	0.09	1.58	27.43	0.11
P316	515	Top of Galway Mound. BMP	51°27.11'	11°45.17'	818	9.46	35.51	0.40	27.46		0.46	0.05	1.55	27.40	0.06
P316	514	N of Galway Mound. BMP	51°27.28'	11°45.19'	842	9.50	35.50	0.35	27.45		0.46	0.11	1.48	27.35	0.09
P316	534	W of Poseidon Mound. BMP	51°27.30'	11°42.63'	875	9.18	35.52	0.43	27.51		0.47	0.04	1.63	27.47	0.05
P316	518	S of Galway Mound. BMP	51°26.65'	11°45.16'	896	8.50	35.50	0.46	27.61		0.46	-0.01	1.82	27.60	0.01
P316	532	Pentilisea Mound. BMP	51°27.18'	11°44.03'	898	8.93	35.53	0.39	27.56		0.47	0.08	1.65	27.48	0.08
P316	516	E of Galway Mound. BMP	51°27.11'	11°44.87'	899	8.93	35.53	0.44	27.55		0.47	0.03	1.70	27.51	0.04
P316	533	W of Poseidon Mound. BMP	51°27.22'	11°43.55'	908	8.78	35.52	0.53	27.58		0.46	-0.06	1.82	27.60	-0.02
P316	513	N of Galway Mound. BMP	51°27.46'	11°45.31'	908	9.46	35.51	0.43	27.46		0.46	0.03	1.57	27.42	0.04

P316	521	E of Galway Mound. BMP	51°26.97'	11°44.46'	920	8.62	35.51	0.38	27.59		0.46	0.08	1.71	27.52	0.07
P316	512	N of Galway Mound. BMP	51°27.60'	11°45.34'	922	9.11	35.52	0.39	27.52		0.47	0.07	1.61	27.45	0.07
P316	520	W of Galway Mound. BMP	51°26.88'	11°45.80'	972	8.50	35.51	0.44	27.61		0.46	0.02	1.79	27.58	0.03
P316	519	W of Galway Mound. BMP	51°26.91'	11°46.15'	986	8.51	35.51	0.44	27.61		0.46	0.02	1.80	27.58	0.03
P316	531	W of Galway Mound. BMP	51°26.44'	11°47.52'	1050	8.81	35.52	0.50	27.58		0.47	-0.03	1.78	27.57	0.00
P316	530	W of Galway Mound. BMP	51°25.99'	11°48.74'	1088	8.21	35.49	0.43	27.64		0.45	0.02	1.85	27.62	0.02

Table S3. a) Zonal mean LGM temperatures (°C) between 10°W and 15°W at 51.875°N ±0.625°N (from PIMP 2 HadCM3M2 data; Braconnot et al. [2007]). **b)** Zonal mean LGM salinities (g kg^{-1}) between 10°W and 15°W at 51.875°N ±0.625°N (from PIMP 2 HadCM3M2 data; Braconnot et al. [2007]). **c)** Zonal mean LGM seawater densities (σ_θ in kg m^{-3}) based on temperature and salinity data from tables S3a and S3b between 10°W and 15°W at 51.875°N ±0.625°N.

a) Depth (m)	JAN	FEB	MAR	APR	MAY	JUN	JUL	AUG	SEP	OCT	NOV	DEC	Annual mean
5	9.43	9.13	9.02	9.14	9.71	10.82	11.81	12.00	11.61	10.93	10.31	9.84	10.31
15	9.43	9.13	9.02	9.13	9.69	10.75	11.76	11.99	11.61	10.93	10.31	9.84	10.30
25	9.43	9.13	9.02	9.13	9.66	10.66	11.67	11.97	11.61	10.93	10.31	9.84	10.28
35.1	9.43	9.13	9.02	9.13	9.62	10.50	11.47	11.90	11.60	10.93	10.31	9.84	10.24
47.85	9.43	9.13	9.02	9.12	9.56	10.26	11.03	11.62	11.57	10.93	10.31	9.84	10.15
67	9.43	9.13	9.02	9.11	9.45	9.93	10.36	10.85	11.24	10.92	10.31	9.84	9.97
95.75	9.43	9.13	9.02	9.08	9.33	9.62	9.84	10.08	10.43	10.68	10.31	9.84	9.73
138.9	9.41	9.12	8.99	9.03	9.18	9.34	9.47	9.61	9.78	10.01	10.11	9.81	9.49
203.7	9.61	9.40	9.30	9.31	9.37	9.42	9.43	9.44	9.48	9.55	9.67	9.75	9.48
301	9.06	9.11	9.11	9.11	9.12	9.10	9.05	9.00	8.96	8.94	8.94	8.98	9.04
447.05	8.01	8.10	8.16	8.21	8.22	8.21	8.16	8.10	8.02	7.95	7.92	7.94	8.08
666.3	6.18	6.35	6.48	6.56	6.55	6.48	6.36	6.23	6.10	6.01	5.99	6.06	6.28
995.55	3.50	3.55	3.60	3.62	3.62	3.60	3.56	3.51	3.48	3.45	3.45	3.47	3.53
1500.85	1.72	1.73	1.73	1.73	1.73	1.73	1.72	1.71	1.71	1.70	1.70	1.71	1.72
2116.15	0.77	0.78	0.79	0.79	0.79	0.79	0.78	0.77	0.76	0.76	0.76	0.76	0.78

b) Depth (m)	JAN	FEB	MAR	APR	MAY	JUN	JUL	AUG	SEP	OCT	NOV	DEC	Annual mean
5	35.25	35.26	35.28	35.29	35.28	35.25	35.20	35.17	35.16	35.17	35.19	35.22	35.23
15	35.25	35.26	35.28	35.29	35.28	35.25	35.20	35.18	35.16	35.17	35.19	35.22	35.23
25	35.25	35.26	35.28	35.29	35.28	35.25	35.21	35.18	35.16	35.17	35.19	35.22	35.23
35.1	35.25	35.26	35.28	35.29	35.28	35.25	35.22	35.18	35.16	35.17	35.19	35.22	35.23
47.85	35.25	35.26	35.28	35.29	35.28	35.26	35.23	35.19	35.17	35.17	35.19	35.22	35.23
67	35.25	35.26	35.28	35.29	35.28	35.26	35.25	35.22	35.19	35.18	35.19	35.22	35.24
95.75	35.25	35.26	35.28	35.29	35.28	35.27	35.27	35.26	35.25	35.21	35.20	35.22	35.25
138.9	35.25	35.27	35.28	35.29	35.29	35.29	35.29	35.29	35.29	35.27	35.24	35.23	35.27
203.7	35.29	35.31	35.32	35.32	35.32	35.31	35.31	35.30	35.30	35.30	35.29	35.29	35.30
301	35.32	35.33	35.34	35.34	35.34	35.33	35.33	35.32	35.32	35.31	35.31	35.31	35.33
447.05	35.31	35.31	35.32	35.33	35.33	35.32	35.32	35.31	35.31	35.31	35.30	35.30	35.31
666.3	35.28	35.28	35.29	35.29	35.29	35.29	35.29	35.29	35.28	35.28	35.28	35.28	35.28
995.55	35.24	35.24	35.24	35.24	35.24	35.24	35.24	35.24	35.24	35.24	35.24	35.24	35.24
1500.85	35.24	35.25	35.25	35.24	35.24	35.24	35.24	35.24	35.24	35.24	35.24	35.24	35.24
2116.15	35.26	35.26	35.26	35.26	35.26	35.26	35.26	35.26	35.26	35.26	35.26	35.26	35.26

c) Depth (m)	JAN	FEB	MAR	APR	MAY	JUN	JUL	AUG	SEP	OCT	NOV	DEC	Annual mean
5	27.24	27.30	27.34	27.32	27.22	27.00	26.78	26.72	26.79	26.92	27.05	27.15	27.08
15	27.24	27.30	27.34	27.33	27.22	27.02	26.79	26.73	26.79	26.92	27.06	27.15	27.08
25	27.24	27.30	27.34	27.34	27.23	27.03	26.82	26.74	26.79	26.92	27.06	27.15	27.08
35.1	27.24	27.30	27.34	27.34	27.24	27.06	26.86	26.75	26.79	26.92	27.06	27.15	27.09
47.85	27.24	27.30	27.34	27.34	27.25	27.11	26.95	26.81	26.80	26.92	27.06	27.15	27.11
67	27.24	27.30	27.34	27.34	27.26	27.17	27.09	26.98	26.88	26.93	27.06	27.15	27.15
95.75	27.24	27.30	27.34	27.34	27.28	27.23	27.19	27.14	27.08	27.00	27.06	27.15	27.19
138.9	27.25	27.31	27.34	27.34	27.32	27.29	27.27	27.25	27.22	27.16	27.12	27.12	27.25
203.7	27.26	27.30	27.32	27.32	27.31	27.29	27.29	27.28	27.28	27.26	27.24	27.22	27.28
301	27.36	27.36	27.37	27.34	27.37	27.36	27.37	27.37	27.38	27.37	27.37	27.37	27.37

447.05	27.52	27.50	27.50	27.50	27.50	27.49	27.50	27.50	27.52	27.53	27.52	27.52	27.51
666.3	27.75	27.73	27.72	27.71	27.71	27.72	27.74	27.75	27.76	27.77	27.78	27.77	27.74
995.55	28.03	28.02	28.02	28.02	28.02	28.02	28.02	28.03	28.03	28.03	28.03	28.03	28.03
1500.85	28.19	28.19	28.19	28.19	28.19	28.19	28.19	28.19	28.19	28.19	28.19	28.19	28.19
2116.15	28.27	28.27	28.27	28.27	28.27	28.27	28.27	28.27	28.27	28.27	28.27	28.27	28.27

Table S4. Stable oxygen isotope [Dorschel et al., 2005] and paleo-density data of core GeoB 6730-1. Equations 1, 6 and 7 correspond to main text. MIS = Marine Isotope Stages (see Fig. 2 and Table 1 of manuscript). Analytical standard deviation for $\delta^{18}O_C$ is ±0.07‰ PDB, for paleo-density reconstruction ±0.1–0.15 kg m^{-3}. Paleo-temperatures were calculated using the equation of Marchitto et al. [2014] on the basis of given paleo-$\delta^{18}O_{sw}$.

Depth (cm)	$\delta^{18}O_c$ (‰)	Paleo-density (kg m^{-3})	Equation No.	Paleo-temperature (°C)	Paleo-$\delta^{18}O_{sw}$ (‰)	MIS
3	1.49	27.29	1	9.7	0.45	1
8	1.42	27.24	1	10.0	0.45	1
13	1.44	27.25	1	9.9	0.45	1
18	1.45	27.26	1	9.9	0.45	1
23	1.50	27.29	1	9.6	0.45	1
28	1.55	27.32	1	9.4	0.45	1
33	1.51	27.29	1	9.6	0.45	1
38	1.48	27.28	1	9.7	0.45	1
43	1.48	27.28	1	9.7	0.45	1
48	1.57	27.33	1	9.3	0.45	1
53	1.53	27.31	1	9.5	0.45	1
58	1.84	27.48	HIATUS	8.1	0.45	HIATUS
63	2.12	27.28	6	8.4	0.8	5
68	2.21	27.32	6	8.1	0.8	5
73	2.34	27.38	6	7.5	0.8	5
78	2.35	27.39	6	7.4	0.8	5
83	2.32	27.37	6	7.6	0.8	5
88	2.27	27.35	6	7.8	0.8	5
93	2.28	27.35	6	7.8	0.8	5
98	2.40	27.41	6	7.2	0.8	5
103	2.22	27.33	6	8.0	0.8	5
108	2.27	27.35	6	7.8	0.8	5
113	2.33	27.38	6	7.5	0.8	5
118	1.95	27.19	HIATUS	9.2	0.8	HIATUS
123	3.04	27.55	7	5.3	1	6.5
128	2.77	27.52	7	6.5	1	6.5
133	3.22	27.56	7	4.6	1	6.5
138	3.32	27.57	7	4.1	1	6.5
143	3.28	27.57	7	4.3	1	6.5
148	3.19	27.56	7	4.7	1	6.5
153	3.36	27.57	7	4.0	1	6.5
158	3.28	27.57	7	4.3	1	6.5
163	3.05	27.55	7	5.3	1	6.5
168	2.85	27.53	7	6.1	1	6.5
173	2.58	27.48	7	7.3	1	6.5
178	2.43	27.45	7	7.9	1	6.5
183	2.36	27.39	6	8.3	1	HIATUS
188	2.51	27.45	6	6.8	0.8	7
193	2.49	27.44	6	6.8	0.8	7
198	2.37	27.40	6	7.3	0.8	7
203	2.27	27.35	6	7.8	0.8	7
208	2.34	27.39	6	7.5	0.8	7
213	2.33	27.38	6	7.5	0.8	7
218	2.35	27.39	6	7.5	0.8	7
223	2.42	27.42	6	7.2	0.8	7
233	2.35	27.39	6	7.4	0.8	7

238	2.25	27.34	6	7.9	0.8	7
243	2.28	27.36	6	7.7	0.8	7
248	2.25	27.34	6	7.9	0.8	7
258	2.02	27.23	6	8.9	0.8	7
263	1.92	27.18	HIATUS	9.3	0.8	HIATUS
268	1.78	27.10	HIATUS	9.9	0.8	HIATUS
278	2.32	27.38	6	7.6	0.8	9
283	2.08	27.26	6	8.6	0.8	9
288	2.25	27.34	6	7.9	0.8	9
293	2.60	27.49	6	6.4	0.8	9
298	2.45	27.43	6	7.0	0.8	9
303	2.59	27.48	HIATUS	6.4	0.8	HIATUS
308	2.53	27.46	6	6.6	0.8	9
313	2.59	27.49	6	6.4	0.8	9
318	2.89	27.59	6	5.1	0.8	9
323	2.98	27.62	6	4.7	0.8	9
328	2.89	27.59	6	5.1	0.8	9
333	2.96	27.61	6	4.8	0.8	9
338	2.74	27.54	6	5.7	0.8	9
343	2.66	27.51	6	6.1	0.8	9
353	3.08	27.64	6	4.3	0.8	9
358	2.65	27.51	6	6.1	0.8	9

Table S5. Stable oxygen isotope [Raddatz et al., 2011] and paleo-density data of IODP 307 Site U1317C. Equation 7 is used for paleo-density reconstruction (see manuscript). Analytical standard deviation for $\delta^{18}O$ is ±0.05‰ PDB, for paleo-density reconstruction ±0.1–0.15 kg m^{-3}. Mbsf = meters below seafloor. Paleo-temperatures were calculated using the equation of Marchitto et al. [2014] on the basis of paleo-$\delta^{18}O_{sw}$ of 0‰ for the Early Pleistocene and –0.25‰ for the Middle Miocene [Zachos et al., 2001]. These data are compared and in accordance to published data of Raddatz et al. [2011, 2014] using other methods.

U1317C-	Depth (mbsf)	$\delta^{18}O_C$ (‰ PDB)*	Paleo-density (kg m^{-3})	Paleo-temperature (°C)
16-7/4.5	141.19	1.88	27.35	10.1
16-7/14.5	141.29	1.79	27.29	10.5
16-7/24.5	141.39	1.80	27.29	10.4
16-7/34.5	141.49	1.83	27.31	10.3
16-7/44.5	141.59	1.85	27.32	10.2
16-7/54.5	141.69	1.69	27.21	10.9
16-7/64.5	141.79	1.86	27.33	10.2
16-7/74.5	141.89	1.80	27.29	10.4
16-7/84.5	141.99	1.74	27.25	10.7
16-7/94.5	142.09	1.81	27.30	10.4
16-7/104.5	142.19	2.00	27.42	9.6
16-7/114.5	142.29	1.81	27.30	10.0
16-8/4.5	142.43	1.89	27.35	10.0
16-8/14.5	142.53	1.95	27.39	9.8
16-8/24.5	142.63	2.02	27.43	9.5
16-8/34.5	142.73	2.17	27.52	8.8
16-8/44.5	142.83	2.11	27.49	9.1
16-8/54.5	142.93	2.22	27.55	8.6
16-8/64.5	143.03	2.14	27.51	9.0
16-ccw/4.5	143.16	2.52	27.71	7.4
16-ccw/14.5	143.26	2.48	27.69	7.5
17-1/4.5	143.35	2.23	27.56	8.6
17-1/14.5	143.45	2.01	27.43	9.5
17-1/24.5	143.55	1.88	27.34	10.1
17-1/34.5	143.65	2.10	27.48	9.1
17-1/44.5	143.75	1.92	27.37	9.9
17-1/54.5	143.85	2.00	27.42	9.6
17-1/64.5	143.95	2.03	27.44	9.5
17-1/74.5	144.05	1.45	27.05	11.9
17-1/84.5	144.15	2.06	27.46	9.3
17-1/94.5	144.25	2.04	27.44	9.4
17-1/104.5	144.35	1.89	27.35	10.1
17-1/114.5	144.45	1.77	27.27	10.6
17-2/4.5	144.56	1.94	27.39	9.8
17-2/14.5	144.66	1.86	27.33	10.2
17-2/24.5	144.76	1.81	27.30	10.4
17-2/44.5	144.96	2.23	27.56	8.6
17-2/54.5	145.06	2.28	27.58	8.4
17-2/64.5	145.16	1.87	27.34	10.1
17-2/74.5	145.26	1.89	27.35	10.1
17-2/84.5	145.36	1.84	27.32	10.3
17-2/104.5	145.56	1.77	27.27	10.6
17-2/114.5	145.66	1.95	27.39	9.8
17-3/6.5	145.79	2.14	27.50	9.0
17-3/13.5	145.86	1.85	27.32	10.2

17-3/20.5	145.93	1.90	27.36	10.0
17-3/27.5	146.00	2.05	27.45	9.4
17-3/34.5	146.07	1.92	27.37	9.9
17-3/48.5	146.21	2.29	27.59	8.3
17-3/55.5	146.28	2.16	27.52	8.9
17-3/61.5	146.34	2.30	27.60	8.3
17-3/97.5	146.70	2.00	27.42	9.6
17-3/104.5	146.77	1.96	27.40	9.7
17-3/111.5	146.84	2.10	27.48	9.1
17-3/118.5	146.91	1.97	27.40	9.7
17-4/6.5	147.02	1.94	27.38	9.8
17-4/13.5	147.09	1.98	27.41	9.7
17-4/20.5	147.16	1.93	27.37	9.9
17-4/26.5	147.22	2.06	27.46	9.3
17-4/32.5	147.28	2.23	27.56	8.6
17-4/41.5	147.37	2.17	27.52	8.8
17-4/48.5	147.44	2.15	27.51	8.9
17-4/55.5	147.51	1.93	27.38	9.9
17-4/62.5	147.58	2.08	27.47	9.2
17-4/69.5	147.65	2.14	27.50	9.0
17-4/76.5	147.72	1.91	27.36	10.0
17-4/85.5	147.81	2.14	27.51	9.0
17-4/90.5	147.86	2.11	27.48	9.1
17-4/96.5	147.92	2.11	27.49	9.1
17-4/111.5	148.07	0.13	25.84	16.8
17-4/118.5	148.14	0.08	25.78	17.0
17-5/4.5	148.20	0.23	25.95	16.3
17-5/14.5	148.30	0.13	25.84	16.8
17-5/34.5	148.50	0.18	25.89	16.6
17-5/44.5	148.60	0.10	25.81	16.9
17-5/54.5	148.70	0.16	25.88	16.6
17-5/64.5	148.80	0.43	26.15	15.4
17-5/74.5	148.90	-0.17	25.51	18.2
17-5/84.5	149.00	0.03	25.74	17.2
17-5/94.5	149.10	0.22	25.94	16.4
17-5/104.5	149.20	0.13	25.84	16.8
17-5/114.5	149.30	0.03	25.73	17.2
17-6/7.5	149.46	0.01	25.71	17.3
17-6/17.5	149.56	0.19	25.90	16.5
17-6/27.5	149.66	-0.02	25.68	17.5
17-6/38.5	149.77	0.11	25.82	16.9
17-6/47.5	149.86	0.15	25.86	16.7
17-6/57.5	149.96	0.08	25.78	17.0
17-6/67.5	150.06	0.11	25.82	16.9
17-6/77.5	150.16	0.26	25.98	16.2
17-6/97.5	150.36	0.08	25.79	17.0
17-6/107.5	150.46	0.20	25.91	16.5
17-6/117.5	150.56	-0.15	25.54	18.1
17-ccw/3.5	150.63	0.19	25.90	16.5
17-ccw/13.5	150.73	0.20	25.92	16.4

Table S6. $\delta^{18}O_C$ ratios of *Cibicidoides kullenbergi* ($\delta^{18}O_{kull}$) and *Cibicidoides wuellerstorfi* ($\delta^{18}O_{wuell}$) of fraction 250 to 500 µm from gravity cores of Propeller Mound. Analytical standard deviation for $\delta^{18}O_C$ is ±0.07‰ PDB.

Core GeoB	Depth (cm)	$\delta^{18}O_{wuell}$ (‰ PDB)	$\delta^{18}O_{kull}$ (‰ PDB)
6729-1	8	3.37	2.71
6729-1	38	2.74	2.84
6729-1	73	2.66	3.06
6729-1	108	2.35	2.34
6729-1	143	2.22	2.77
6729-1	153	2.80	2.89
6729-1	218	2.32	2.55
6729-1	268	2.56	2.54
6729-1	278	2.62	2.56
6729-1	333	2.14	2.26
6729-1	358	2.52	2.31
6729-1	418	3.32	3.05
6728-1	18	3.16	3.23
6728-1	103	2.35	2.93
6728-1	208	2.67	2.70
6728-1	318	2.41	2.91
6728-1	323	2.40	2.29
6728-1	423	2.84	2.85
6728-1	523	2.55	2.75
6727-1	18	3.46	3.78
6727-1	53	3.70	3.66
6727-1	118	3.65	3.68
6727-1	123	3.69	3.64
6727-1	143	3.39	3.60
6727-1	168	3.44	3.66
6727-1	208	3.53	3.61
6727-1	228	3.30	3.33
6727-1	253	2.67	2.82
6725-1	43	3.68	3.71
6725-1	88	3.62	3.72
6725-1	243	3.68	3.45
6725-1	348	3.40	3.39
6725-1	408	2.79	3.10
6725-1	448	2.37	2.77
6718-2	103	3.38	3.50
6718-2	218	3.83	3.84
6718-2	223	3.67	3.89
6718-2	228	3.68	3.73
6718-2	313	3.68	3.64
6718-2	423	3.59	3.73
6718-2	428	3.64	3.68